

See discussions, stats, and author profiles for this publication at: <https://www.researchgate.net/publication/11682456>

# Metallo 2,3-Disulfidothienoquinoxaline, 2,3-Disulfidothienopyridine, and 2-Sulfido-3-oxidothienoquinoxaline Complexes: Synthesis and Characterization

ARTICLE *in* INORGANIC CHEMISTRY · JUNE 1997

Impact Factor: 4.76 · DOI: 10.1021/ic961428v · Source: PubMed

---

CITATIONS

17

---

READS

11

7 AUTHORS, INCLUDING:



**Anthony Vodacek**

Rochester Institute of Technology

81 PUBLICATIONS 1,653 CITATIONS

SEE PROFILE



**Glenn P. A. Yap**

University of Delaware

634 PUBLICATIONS 14,317 CITATIONS

SEE PROFILE



**Arnold Rheingold**

University of California, San Diego

2,176 PUBLICATIONS 51,628 CITATIONS

SEE PROFILE

# Metallo 2,3-Disulfidothienoquinoxaline, 2,3-Disulfidothienopyridine, and 2-Sulfido-3-oxidothienoquinoxaline Complexes: Synthesis and Characterization

Sharada P. Kaiwar,<sup>†</sup> John K. Hsu,<sup>†</sup> Anthony Vodacek,<sup>†</sup> Glenn Yap,<sup>‡</sup> Louise M. Liable-Sands,<sup>‡</sup> Arnold L. Rheingold,<sup>‡</sup> and Robert S. Pilato<sup>\*,†</sup>

Department of Chemistry and Biochemistry, University of Maryland, College Park, Maryland 20742, and Department of Chemistry, University of Delaware, Newark, Delaware 19711

Received November 27, 1996<sup>®</sup>

The 2,3-disulfidothienoquinoxaline complexes of  $\text{Cp}_2\text{Mo}$  and  $\text{dppePd}$  and the 2,3-disulfidothienopyridine complexes of  $\text{Cp}_2\text{Mo}$  were obtained as products from the  $\text{S}_8$  oxidation of the corresponding metallo-1,2-enedithiolate complexes. The analogous 2-sulfido-3-oxidothienoquinoxaline complexes of  $\text{Cp}_2\text{Ti}$ ,  $\text{Cp}_2\text{Mo}$ ,  $\text{dppPd}$ , and  $\text{dppePt}$  were prepared from 1-(quinoxalin-2-yl)-2-bromoethanone and the corresponding polysulfido complex. Both  $\text{Cp}_2\text{Mo}\{\text{S}_2\text{C}_{10}\text{H}_4\text{N}_2\text{S}\}$  and  $\text{Cp}_2\text{Mo}\{\text{SOC}_{10}\text{H}_4\text{N}_2\text{S}\}$  have been characterized crystallographically. These complexes contain an extended planar ring where the metal is bound to substituents at the 2- and 3-positions of the thiophene ring. The oxidation products of the  $\text{Cp}_2\text{Mo}$  derivatives all have EPR  $g$  values near 1.98 and  $^{97/95}\text{Mo}$  hyperfine of  $\leq 8.5$  G. All of the complexes have a visible band assigned to an intraligand transition (IL). The excitation of a room-temperature DMSO solution of  $\text{dppePt}\{\text{SOC}_{10}\text{H}_4\text{N}_2\text{S}\}$  leads to an emission at 690 nm with a  $\phi = 0.005$ . Lifetime measurements were best fit as the sum of two exponential decays with lifetimes of 6 and 0.3 ns.

## Introduction

Metallo-1,2-enedithiolates,  $\text{M}\{\text{S}_2\text{C}_2(\text{R})(\text{R}')\}$ , have been used as models for the molybdenum cofactor,<sup>1–5</sup> as components in conducting materials,<sup>6–9</sup> and, in the case of platinum-1,2-enedithiolates, as room-temperature solution lumiphores.<sup>10–13</sup> While there are many reasons to study metallo-1,2-enedithiolates, few studies have focused on the reactivity of the metal-bound ligand. While many 1,2-enedithiolate complexes undergo reversible one electron oxidation of the metal or ligand, those complexes with  $\text{R} = \text{H}$  should undergo chemical oxidation. In this paper, the reactions of complexes containing  $\text{R} = \text{H}$  and  $\text{R}' = \text{heterocycle}$ <sup>14,15</sup> with  $\text{S}_8$  are described. The products from these reactions are metallo-2,3-disulfidothiophenes. These complexes were the result of a formal oxidation of both the 1,2-enedithiolate ligand and the appended heterocycle. This

oxidation was accompanied by the formation of a five-membered thiophene ring. The analogous metallo-2-sulfido-3-oxidothiophenes were available from the reaction of a polysulfido complex with the  $\alpha$ -bromo ketone, 1-(quinoxalin-2-yl)-2-bromoethanone.

The synthesis of several metal derivatives of 2,3-disulfidothienoquinoxaline, 2,3-disulfidothienopyridine, and 2-sulfido-3-oxidothienoquinoxaline are described, and an overview of the chemistry of these metal complexes is provided. The rather unique features of these complexes include ligand-centered oxidation, low-lying ligand-centered electronic transitions, and luminescent Pt derivatives.

## Experimental Section

**Materials.**  $\text{Cp}_2\text{Mo}\{\text{S}_2\text{C}_2(2\text{-quinoxaline})(\text{H})\}$ ,<sup>14</sup>  $\text{Cp}_2\text{Mo}\{\text{S}_2\text{C}_2(2\text{-pyridine})(\text{H})\}$ ,<sup>14</sup>  $\text{Cp}_2\text{Mo}\{\text{S}_2\text{C}_2(3\text{-pyridine})(\text{H})\}$ ,<sup>14</sup>  $\text{Cp}_2\text{Mo}\{\text{S}_2\text{C}_2(4\text{-pyridine})(\text{H})\}$ ,<sup>14</sup>  $\text{dppeM}\{\text{S}_2\text{C}_2(2\text{-quinoxaline})(\text{H})\}$  ( $\text{M} = \text{Pd}, \text{Pt}$ ;  $\text{dppe} = \text{diphenyldiphosphinoethane}$ ),<sup>15</sup>  $\text{Cp}_2\text{MoS}_4$ ,<sup>16</sup>  $\text{dppePdS}_4$ ,<sup>17</sup>  $\text{dppePtS}_4$ ,<sup>17</sup>  $\text{Cp}_2\text{TiS}_5$ ,<sup>18</sup>  $\text{Cp}_2\text{Mo}(\text{SH})_2$ ,<sup>19</sup>  $\text{dppePd}(\text{SH})_2$ ,<sup>20</sup> and 1-(quinoxalin-2-yl)-2-bromoethanone<sup>21</sup> were prepared according to the literature procedures. The 54%

<sup>†</sup> University of Maryland.

<sup>‡</sup> University of Delaware.

<sup>®</sup> Abstract published in *Advance ACS Abstracts*, May 1, 1997.

- (1) Pilato, R. S.; Gea, Y.; Eriksen, K. A.; Greaney, M. A.; Stiefel, E. I.; Goswami, S.; Kilpatrick, L.; Spiro, T. G.; Taylor, E. C.; Rheingold, A. L. In *ACS Symposium Series, Molybdenum Enzymes, Cofactors, and Models Systems*; Stiefel, E. I., Coucouvanis, D., Newton, W. E., Eds.; American Chemical Society: Washington, DC, 1993; Vol. 635; pp 83–97.
- (2) (a) Subramanian, P.; Burgmayer, S.; Richards, S.; Szalai, V.; Spiro, T. G. *Inorg. Chem.* **1990**, *29*, 3849–53. (b) Soricelli, C. L.; Szalai, V. A.; Burgmayer, S. J. *N. J. Am. Chem. Soc.* **1991**, *113*, 9877–8.
- (3) Das, S. K.; Chaudhury, P. K.; Biswas, D.; Sarkar, S. *J. Am. Chem. Soc.* **1994**, *116*, 9061–70.
- (4) Kilpatrick, L.; Rajagopalan, K. V.; Hilton, J.; Bastian, N. R.; Stiefel, E. I.; Pilato, R. S.; Spiro, T. G. *Biochemistry* **1995**, *34*, 3032–9.
- (5) Ueyama, N.; Oku, H.; Kondo, M.; Okamura, T.; Yoshinaga, N.; Nakamura, A. *Inorg. Chem.* **1995**, *35*, 643–50.
- (6) Veldhuizen, Y. S. J.; Veldman, N.; Spek, A. L.; Faulmann, C.; Haasnoot, J. G.; Reedijk, J. *Inorg. Chem.* **1995**, *34*, 140–7.
- (7) Fournigue, M.; Lenoir, C.; Coulon, C.; Guyon, F.; Amaudrut, J. *Inorg. Chem.* **1995**, *34*, 4979–4985.
- (8) Schrauzer, G. N. *Acc. Chem. Res.* **1969**, *2*, 72–80.
- (9) Clemenson, P. I. *Coord. Chem. Rev.* **1990**, *106*, 171–203.
- (10) Cummings, S. D.; Eisenberg, R. *J. Am. Chem. Soc.* **1996**, *118*, 1949–60.
- (11) Cummings, S. D.; Eisenberg, R. *Inorg. Chem.* **1995**, *34*, 3396–403.
- (12) Bevilacqua, M. J.; Eisenberg, R. *Inorg. Chem.* **1994**, *33*, 2913–23.
- (13) Kaiwar, S. P.; Vodacek, A.; Blough, N. V.; Pilato, R. S. *J. Am. Chem. Soc.* **1997**, *119*, 3311–16.

- (14) (a) Hsu, J. K.; Bonangelino, C. J.; Kaiwar, S. P.; Boggs, C. M.; Fetting, J. C.; Pilato, R. S. *Inorg. Chem.* **1996**, *35*, 4743–51. (b) Kaiwar, S. P.; Hsu, J. K.; Liable-Sands, L. M.; Rheingold, A. L.; Pilato, R. S. The Synthesis of Heterocyclic Substituted-1,2-enedithiolates of Nickel, Palladium, and Platinum. Submitted for publication.
- (15) Kaiwar, S. P.; Vodacek, A.; Blough, N. V.; Pilato, R. S. Protonation State Dependent Luminescence and Excited State Electron Transfer Reactions of 2- and 4-Pyridine(ium) Substituted Metallo-1,2-enedithiolates. Submitted for publication.
- (16) Köpf, H.; Kahl, W.; Wirl, A. *Angew. Chem., Int. Ed. Engl.* **1970**, *9*, 801–2.
- (17) Chatt, J.; Mingos, D. M. P. *J. Chem. Soc. A* **1970**, 1243–5.
- (18) McCall, J. M.; Shaver, A. *J. Organomet. Chem.* **1980**, *193*, C37–C39.
- (19) Green, M. L. H.; Lindsell, W. E. *J. Chem. Soc. A* **1967**, 1455.
- (20) (a) Schmidt, M.; Hoffmann, G. G.; Holler, R. *Inorg. Chim. Acta* **1979**, *32*, L19–L20. The  $^1\text{H}$  NMR resonance for the hydrosulfido ligands of **3** was improperly assigned: **3**,  $(\text{dppe})\text{Pd}(\text{SH})_2$ :  $^1\text{H}$  NMR ( $\text{CDCl}_3$ )  $\delta$  –0.55 (second-order multiplet, 2H, SH, line spacings = 11 and 6 Hz).
- (21) (a) Rowe, D. J.; Garner, C. D.; Joule, J. A. *J. Chem. Soc., Perkin Trans. 1* **1985**, 1907–10. (b) Gardini, G. P.; Minisci, F. *J. Chem. Soc. C* **1970**, 929.

HB $F_4$  etherate was purchased from Fluka Chemika and was used as received. All reactions were performed under an atmosphere of nitrogen using standard Schlenk line techniques. Neutral activated alumina, 80–325 mesh, was purchased from EM Science, Cherry Hill, NJ, and treated with 6% H $_2$ O by weight to generate the Brockmann activity 3 material used throughout the study. Workups were performed in air unless stated otherwise. Dichloromethane, acetonitrile, and pentane were dried over calcium hydride and distilled under nitrogen. Diethyl ether, tetrahydrofuran, and dioxane were dried over sodium/benzophenone and distilled under nitrogen. Triethylamine was dried over potassium hydroxide and vacuum distilled.

**Physical Measurements.** NMR measurements were made on either a Bruker AF 200 or a Bruker AM 400. EPR measurements were made on a Bruker ES-D 200. UV–vis measurements were made on a Perkin-Elmer  $\lambda$ -2S UV–visible spectrometer. IR spectra were collected on either a Perkin-Elmer 1600 Series FT-IR spectrometer or a Nicolet 5 DXL FT-IR spectrometer. Mass spectral data were collected on a Magnetic Sector VG 7070E. All electrochemical experiments were conducted on a BAS-50 in either CV or OSW modes with 0.1 M [Bu $_4$ N] $^{+}$ [PF $_6$ ] $^{-}$  as the supporting electrolyte. In all electrochemical experiments, the electrodes used were a carbon working, platinum auxiliary, and Ag/AgCl reference. Under these conditions, the ferrocene/ferrocenium couple (DMF) was found at 511 mV. All values reported in the text are relative to SCE and were adjusted using the ferrocene/ferrocenium couple. Chemical analyses were performed by M-H-W Laboratories, Phoenix, Az.

**Synthetic Procedures.** **Cp $_2$ Mo{S $_2$ C $_{10}$ H $_4$ N $_2$ S} (9).** To a DMF solution (3 mL) of Cp $_2$ Mo{S $_2$ C $_2$ (2-quinoxaline)(H)} (0.050 g, 0.112 mmol) was added S $_8$  (0.0070 g, 0.027 mmol) and 54% HBF $_4$  etherate (0.1 mL). The reaction was heated for 12 h at 90 °C. The purple solution was cooled, and NEt $_3$  was added dropwise until the solution became red. The DMF was removed in vacuo, and the solid was chromatographed in air on a 2  $\times$  15 cm alumina column. The product, **9**, eluted with 1:4 pentane/dichloromethane and was obtained as a red solid in 67% yield (0.036 g, 0.082 mmol) upon the removal of the eluent. Anal. Calcd for C $_{20}$ H $_{14}$ N $_2$ S $_3$ Mo: C, 50.63; H, 2.95; N, 5.91. Found: C, 50.51; H, 3.24; N, 5.69.  $^1$ H NMR (CD $_2$ Cl $_2$ ):  $\delta$  8.00 (m, 1H, C $_8$ H $_4$ N $_2$ ), 7.63 (m, 1H, C $_8$ H $_4$ N $_2$ ), 7.23 (m, 1H, C $_8$ H $_5$ N $_2$ ), 7.15 (m, 1H, C $_6$ H $_4$ ), 5.43 (s, 10H, C $_5$ H $_5$ ). Mass spectrum [ $m/z$  (EI)]: 476 (M $^{+}$ ), 228 (M $^{+}$  – C $_{10}$ H $_4$ N $_2$ S $_3$ ). UV–vis [(abs) CH $_2$ Cl $_2$ , nm;  $\lambda_{\max}$  (e)]: 334 (13 825), 371 (sh) (6017), 532 (3541).

**dppePd{S $_2$ C $_{10}$ H $_4$ N $_2$ S} (10).** To a DMF solution (3 mL) of dppePd{S $_2$ C $_2$ (2-quinoxaline)(H)} (0.066 g, 0.100 mmol) was added S $_8$  (0.0080 g, 0.031 mmol) and 54% HBF $_4$  etherate (0.1 mL). The solution was heated to 90 °C for 24 h. The DMF was removed under vacuum, and the solid was dissolved in dichloromethane and washed with water. The dichloromethane was removed in vacuo, and the solid was chromatographed in air on a 1  $\times$  20 cm alumina column. The column was eluted with 1:2 hexane/dichloromethane, and **10** was isolated as a red solid in 48% yield (0.036 g, 0.048 mmol) upon the removal of the eluent. Anal. Calcd for C $_{36}$ H $_{28}$ N $_2$ P $_2$ S $_3$ Pd: C, 57.45; H, 3.72; N, 3.72. Found: C, 57.30; H, 3.74; N, 3.39.  $^1$ H NMR (CDCl $_3$ ):  $\delta$  8.17–8.15 (m, 1H, C $_{10}$ H $_4$ N $_2$ ), 7.96–7.93 (m, 1H, C $_{10}$ H $_4$ N $_2$ ), 7.90–7.84 (m, 1H, C $_8$ H $_5$ N $_2$ ), 7.83–7.76 (m, 8H, C $_6$ H $_5$ P), 7.60–7.57 (m, 1H, C $_8$ H $_5$ N $_2$ ), 7.55–7.41 (m, 12H, C $_6$ H $_5$ P), 2.63–2.47 (m, 4H, PC $_2$ H $_2$ ).  $^{31}$ P{ $^1$ H} NMR (CDCl $_3$ ): 55.47 (d,  $J_{P-P}$  = 27 Hz), 53.86 (d,  $J_{P-P}$  = 27 Hz). Mass spectrum [ $m/z$  (FAB)]: 753 (M $^{+}$ ), 504 (M $^{+}$  – C $_{10}$ H $_4$ S $_3$ N $_2$ ). UV–vis [(abs) CH $_2$ Cl $_2$ , nm;  $\lambda_{\max}$  (e)]: 326 (10280), 376 (6820), 476 (5610).

**Cp $_2$ Mo{S $_2$ C $_3$ H $_3$ NS}·0.5CH $_2$ Cl $_2$  (11, 12).** To a DMF solution (3 mL) of Cp $_2$ Mo{S $_2$ C $_2$ (3-pyridine)(H)} (0.058 g, 0.148 mmol) was added S $_8$  (0.010 g, 0.04 mmol) and 54% HBF $_4$  etherate (0.1 mL). The solution was heated to 90 °C for 12 h. To the cooled red solution was added several drops of NEt $_3$ . The solvent was removed in vacuo, and the solid was chromatographed in air on a 1  $\times$  20 cm alumina column. The column was eluted with 1:4 pentane/dichloromethane to yield **12** in 24% yield (0.016 g, 0.035 mmol) upon the removal of the eluent. The column was then eluted with dichloromethane to yield **11** in 15% yield (0.010 g, 0.022 mmol) upon the removal of the eluent. Both compounds are red crystalline solids that consistently included a  $1/2$  molecule of CH $_2$ Cl $_2$  as determined by  $^1$ H NMR and elemental analysis.

**11.** Anal. Calcd for C $_{17.5}$ H $_{14}$ NS $_3$ MoCl: C, 45.12; H, 3.03; N, 3.01. Found: C, 45.24; H, 3.28; N, 2.78.  $^1$ H NMR (CDCl $_3$ ):  $\delta$  8.64 (s, 1H, C $_5$ H $_3$ N), 8.17 (d, 1H, C $_5$ H $_3$ N,  $J_{H-H}$  = 6 Hz), 7.37 (d, 1H, C $_5$ H $_3$ N,  $J_{H-H}$  = 6 Hz), 5.39 (s, 10H, C $_5$ H $_5$ ). Mass spectrum [ $m/z$  (EI)]: 425 (M $^{+}$ ), 360 (M $^{+}$  – C $_5$ H $_5$ ), 228 (M $^{+}$  – C $_7$ H $_3$ S $_3$ N). UV–vis [(abs) CH $_2$ Cl $_2$ , nm;  $\lambda_{\max}$  (e)]: 358 (3950), 529 (660).

**12.** Anal. Calcd for C $_{17.5}$ H $_{14}$ NS $_3$ MoCl: C, 45.12; H, 3.03; N, 3.01. Found: C, 45.52; H, 3.32; N, 2.83.  $^1$ H NMR (CDCl $_3$ ):  $\delta$  8.20 (d, 1H, C $_5$ H $_3$ N,  $J_{H-H}$  = 5 Hz), 7.60 (d, 1H, C $_5$ H $_3$ N,  $J_{H-H}$  = 8 Hz), 7.12 (dd, 1H, C $_5$ H $_3$ N,  $J_{H-H}$  = 5 Hz;  $J_{H-H}$  = 8 Hz), 5.39 (s, 10H, C $_5$ H $_5$ ). Mass spectrum [ $m/z$  (EI)]: 425 (M $^{+}$ ), 360 (M $^{+}$  – C $_5$ H $_5$ ), 228 (M $^{+}$  – C $_7$ H $_3$ S $_3$ N). UV–vis [(abs) CH $_2$ Cl $_2$ , nm;  $\lambda_{\max}$  (e)]: 296 (7900), 376 (3110), 531 (820).

**Cp $_2$ Mo{S $_2$ C $_3$ H $_3$ NS} (13).** Complexes **13** was prepared as described for **11** and **12** using Cp $_2$ Mo{S $_2$ C $_2$ (2-pyridine)(H)} (0.070 g, 0.178 mmol) in place of Cp $_2$ Mo{S $_2$ C $_2$ (3-pyridine)(H)} and S $_8$  (0.012 g, 0.045 mmol). Complex **13** was isolated as a purple solid in 4% yield (0.003 g, 0.007 mmol) upon eluting the column with dichloromethane and the removal of the eluent.  $^1$ H NMR (CDCl $_3$ ):  $\delta$  8.46 (d, 1H, C $_5$ H $_3$ N,  $J_{H-H}$  = 6 Hz), 7.68 (d, 1H, C $_5$ H $_3$ N,  $J_{H-H}$  = 6 Hz), 7.89 (dd, 1H, C $_5$ H $_3$ N,  $J_{H-H}$  = 6 Hz,  $J_{H-H}$  = 6 Hz), 5.39 (s, 10H, C $_5$ H $_5$ ). Mass spectrum [ $m/z$  (EI)]: 425 (M $^{+}$ ), 360 (M $^{+}$  – C $_5$ H $_5$ ), 228 (M $^{+}$  – C $_7$ H $_3$ S $_3$ N). UV–vis [(abs) CH $_2$ Cl $_2$ , nm;  $\lambda_{\max}$  (e)]: 378 (3890), 521 (1050).

**Cp $_2$ Mo{SOC $_{10}$ H $_4$ N $_2$ S} (19).** To a DMF solution (5 mL) of Cp $_2$ MoS $_4$  (0.175 g, 0.50 mmol) was added 1-(quinoxalin-2-yl)-2-bromoethanone (0.378 g, 1.50 mmol). The reaction mixture was heated at 90 °C for 30 min to give a violet solution. The DMF was removed, and the solid was washed with 3  $\times$  20 mL of diethyl ether. The solid was dissolved in dichloromethane (3 mL) to which three drops of triethylamine was added to give a purple-red solution. The solvent was removed in air, and the solid was chromatographed on a 1  $\times$  20 cm alumina column. Complex **19** was isolated as a purple solid in 57% yield (0.131 g, 0.285 mmol) upon eluting the column with 1:2 hexane/dichloromethane and the removal of the eluent. Crystallization from dichloromethane/pentane gave analytically pure material. Anal. Calcd for C $_{20}$ H $_{14}$ N $_2$ OS $_2$ Mo: C, 52.40; H, 3.06; N, 6.11. Found: C, 52.23; H, 3.30; N, 6.29.  $^1$ H NMR (CD $_2$ Cl $_2$ ):  $\delta$  7.92 (m, 1H, C $_8$ H $_4$ N $_2$ ), 7.54 (m, 1H, C $_8$ H $_4$ N $_2$ ), 7.23 (m, 1H, C $_8$ H $_5$ N $_2$ ), 7.15 (m, 1H, C $_8$ H $_4$ N $_2$ ), 5.58 (s, 10H, C $_5$ H $_5$ ). Mass spectrum [ $m/z$  (EI)]: 460 (M $^{+}$ ), 228 (M $^{+}$  – C $_{10}$ H $_4$ N $_2$ OS $_2$ ). UV–vis [(abs) CH $_2$ Cl $_2$ , nm;  $\lambda_{\max}$  (e)]: 332 (15053), 536 (3508).

**Cp $_2$ Ti{SOC $_{10}$ H $_4$ N $_2$ S} (20).** To a DMF (5 mL) solution of Cp $_2$ TiS $_5$  (0.030 g, 0.100 mmol) was added 1-(quinoxalin-2-yl)-2-bromoethanone (0.075 g, 0.300 mmol). The reaction mixture was heated at 90 °C for 2 h to give a purple solution. The DMF was removed, and the solid was washed with three 20 mL portions each of pentane, diethyl ether, and CCl $_4$ . The black solid was dissolved in CH $_2$ Cl $_2$  to give a purple solution that was washed with H $_2$ O until the CH $_2$ Cl $_2$  was orange-red. The CH $_2$ Cl $_2$  was removed in vacuo to give **20** in 42% yield (0.052 g, 0.124 mmol) as an orange solid.  $^1$ H NMR (CDCl $_3$ ):  $\delta$  8.17–8.11 (m, 2H, C $_{10}$ H $_4$ N $_2$ ), 7.86–7.79 (m, 2H, C $_{10}$ H $_4$ N $_2$ ), 6.62 (s, 10H, 2C $_5$ H $_5$ ). High-resolution mass spectra (EI): Calcd for C $_{20}$ H $_{14}$ OS $_2$ N $_2$ Ti,  $m/z$  410.002 72; found,  $m/z$  410.003 59. UV–vis [(abs) CH $_2$ Cl $_2$ , nm;  $\lambda_{\max}$  (e)]: 328 (8320), 429 (1840), 482 (sh 1000), 562 (sh 340).

**dppePd{SOC $_{10}$ H $_4$ N $_2$ S} (21).** To a DMF solution (5 mL) of dppePdS $_4$  (0.126 g, 0.200 mmol) was added 1-(quinoxalin-2-yl)-2-bromoethanone (0.151 g, 0.600 mmol), and the reaction mixture was heated at 90 °C in an oil bath for 30 min to give a violet solution. The DMF was removed under vacuo, and the solid was dissolved in dichloromethane and washed with water. The dichloromethane was removed in vacuo, and the solid was chromatographed in air on a 1  $\times$  20 cm alumina column. **21** was isolated as a red solid in 51% yield (0.075 g, 0.102 mmol) upon eluting the column with 1:2 hexane/dichloromethane and the removal of the eluent. Crystallization from CH $_2$ Cl $_2$ /pentane gave analytically pure material. Anal. Calcd for C $_{36}$ H $_{28}$ N $_2$ OP $_2$ S $_2$ Pd: C, 58.70; H, 3.80; N, 3.80. Found: C, 58.79; H, 4.10; N, 3.69.  $^1$ H NMR (CD $_2$ Cl $_2$ ):  $\delta$  8.10–8.09 (m, 1H, C $_{10}$ H $_4$ N $_2$ ), 8.07–8.04 (m, 4H, C $_6$ H $_5$ P), 7.94–7.92 (m, 1H, C $_{10}$ H $_4$ N $_2$ ), 7.90–7.88 (m, 1H, C $_8$ H $_5$ N $_2$ ), 7.87–7.81 (m, 4H, C $_6$ H $_5$ P), 7.62–7.60 (m, 1H, C $_8$ H $_5$ N $_2$ ), 7.59–7.50 (m, 12H, C $_6$ H $_5$ P), 2.73–2.42 (m, 4H, PC $_2$ H $_2$ ).  $^{31}$ P{ $^1$ H} NMR (CD $_2$ Cl $_2$ ): 58.86 (d,  $J_{P-P}$  = 22 Hz), 49.19 (d,  $J_{P-P}$  = 22 Hz). Mass spectrum [ $m/z$  (FAB)]: 737 (M $^{+}$ ), 504 (M $^{+}$  – C $_{10}$ H $_4$ OS $_2$ N $_2$ ).

UV-vis [(abs) CH<sub>2</sub>Cl<sub>2</sub>, nm;  $\lambda_{\text{max}}$  ( $\epsilon$ ): 332 (30 590), 358 sh (9380), 370 sh (6470), 518 (5420).

**dppePt{SOC<sub>10</sub>H<sub>4</sub>N<sub>2</sub>S} (22).** This was prepared as described for **21** by replacing dppePdS<sub>4</sub> with dppePtS<sub>4</sub> (0.075 g, 0.100 mmol) and using 1-(quinoxalin-2-yl)-2-bromoethanone (0.075 g, 0.300 mmol). Complex **22** was isolated in 46% yield (0.038 g, 0.051 mmol) as a red solid. Anal. Calcd for C<sub>36</sub>H<sub>28</sub>N<sub>2</sub>O<sub>2</sub>P<sub>2</sub>S<sub>2</sub>Pt: C, 52.36; H, 3.39; N, 3.39. Found: C, 52.47; H, 3.70; N, 3.22. <sup>1</sup>H NMR (CD<sub>2</sub>Cl<sub>2</sub>):  $\delta$  8.11–8.10 (m, 1H, C<sub>10</sub>H<sub>4</sub>N<sub>2</sub>), 8.09–8.05 (m, 4H, C<sub>6</sub>H<sub>5</sub>P), 7.97–7.95 (m, 1H, C<sub>10</sub>H<sub>4</sub>N<sub>2</sub>), 7.88–7.85 (m, 1H, C<sub>8</sub>H<sub>5</sub>N<sub>2</sub>), 7.86–7.81 (m, 4H, C<sub>6</sub>H<sub>5</sub>P), 7.65–7.62 (m, 1H, C<sub>8</sub>H<sub>5</sub>N<sub>2</sub>), 7.58–7.50 (m, 12H, C<sub>6</sub>H<sub>5</sub>P), 2.63–2.39 (m, 4H, PC<sub>2</sub>H<sub>2</sub>). <sup>31</sup>P{<sup>1</sup>H} NMR (CD<sub>2</sub>Cl<sub>2</sub>): 42.31 (d with platinum satellites,  $J_{\text{P-P}} = 12$  Hz,  $J_{\text{P-Pt}} = 2170$ ), 34.17 (d with platinum satellites,  $J_{\text{P-P}} = 12$  Hz,  $J_{\text{P-Pt}} = 2110$ ). Mass spectrum [ $m/z$  (FAB)]: 826 (M<sup>+</sup>), 597 (M<sup>+</sup> – C<sub>10</sub>H<sub>4</sub>N<sub>2</sub>OS<sub>2</sub>). UV-vis [(abs) CH<sub>2</sub>Cl<sub>2</sub>, nm;  $\lambda_{\text{max}}$  ( $\epsilon$ ): 327 (32 700), 357 sh (9410), 370 sh (8150), 501 (6270).

**Structural Determination of Cp<sub>2</sub>Mo{S<sub>2</sub>C<sub>10</sub>H<sub>4</sub>N<sub>2</sub>S} (9).** Crystal, data collection, and refinement parameters are given in Table 1. The systematic absences in the diffraction data are uniquely consistent for the reported space group. The structure was solved using direct methods, completed by subsequent difference Fourier syntheses, and refined by full-matrix least-squares procedures. Semi-empirical absorption corrections were not required because of the <10% variation in the integrated  $\psi$ -scan intensities. All non-hydrogen atoms were refined with anisotropic displacement coefficients. Hydrogen atoms were treated as idealized contributions.

All software and sources of the scattering factors are contained in the SHELXTL 5.3 program library.<sup>22</sup>

**Structural Determination of Cp<sub>2</sub>Mo{SOC<sub>10</sub>H<sub>4</sub>N<sub>2</sub>S} (19).** Crystallographic data are collected in Table 1. Crystals were photographically characterized and determined to belong to the orthorhombic crystal system. Systematic absences in the diffraction data uniquely determined the space group. Azimuthal scans indicated that no correction for absorbance was required;  $T_{\text{max}}/T_{\text{min}} < 1.1$ . The structure was solved by direct methods, completed from difference Fourier maps, and refined with anisotropic thermal parameters for all non-hydrogen atoms except those associated with the Cp rings to conserved data. Hydrogen atom contributions were idealized. All computations used SHELXTL 5.3 software.<sup>22</sup> Attempts to solve the structure as a racemic twin did not improve the refinement.

**Luminescence Measurements of 22.** Room-temperature excitation and emission spectra were acquired with a SLM AB2 fluorescence spectrometer. Emission spectra were corrected for instrumental response using factors supplied by the manufacturer. Luminescence measurements were made on 10<sup>–5</sup> M solutions of **22** (see eq 6) that were deoxygenated by three freeze–pump–thaw N<sub>2</sub>-backfill cycles in a fluorescence cell equipped with a reservoir and a Teflon valve. Quantum yields,  $\phi_s$ , were calculated relative to Zn(tpp) { $\phi_{\text{std}} = 0.04$ }<sup>23</sup> (tpp = tetraphenylporphyrinato) under Ar using eq 1, where  $F$  is the

$$\phi_s = \frac{F_s A_{\text{std}} \eta_s^2 \phi_{\text{std}}}{F_{\text{std}} A_s \eta_{\text{std}}^2} \quad (1)$$

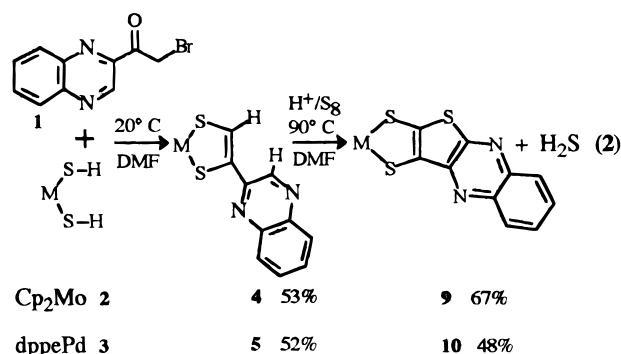
integrated luminescence,  $A$  is the absorbance at the excitation wavelength, and  $\eta$  is the refractive index of the solvent. The subscripts “s” and “std” refer to the sample and the standard, Zn(tpp), respectively.

The lifetimes of **22** were determined with an ISS K2 digital frequency-domain spectrofluorometer. The excitation source was a 300 W Xenon lamp, and the bandpass of the excitation monochromator was 16 nm. Sample and reference solutions were contained in 1 cm quartz cells at room temperature. A scattering solution of glycogen in Milli-Q water was used as the reference for **22**. Single channel detection at 90° was employed, with longpass filters used to block the excitation line and Raman scatter from the sample. Lifetimes were determined from the frequency dependence of the signal phase shifts and demodulation, relative to the reference, using the ISS least-squares analysis software. The minimization procedure assumed discrete

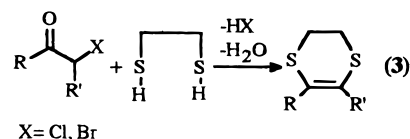
lifetimes. The procedure provided lifetimes, fractional photon contributions, and  $\chi^2$  for the least-squares fit.

## Results and Discussion

It was found that the 2,3-disulfidothienoquinoxaline (DSTQ) complexes, **9** and **10**, could be prepared in two steps from 1-(quinoxalin-2-yl)-2-bromoethanone, **1** (eq 2). The metallo-



1,2-enedithiolates, **4** and **5**, are generated in the first step. The synthesis of **4** and **5** is a nonredox process that is similar to the synthesis of organic-1,4-dithiins from  $\alpha$ -substituted ketones and dimercaptanes (eq 3).<sup>24</sup> The details of the synthesis of **4** and **5**



have been described elsewhere.<sup>14,15</sup> In the second step (eq 2), complexes **4** and **5** were treated with S<sub>8</sub> under acidic conditions to produce the disulfidothienoquinoxaline complexes **9** and **10**. These complexes are air stable in solution and were purified by column chromatography.

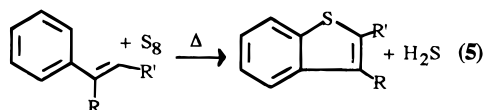
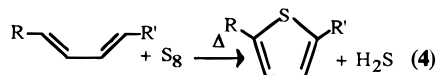
The formation of the DSTQ complexes requires a four-electron oxidation of the 1,2-enedithiolate complex that is accompanied by the loss of two protons. The electrons are transferred to sulfur generating both the thiolate of the thiophene and H<sub>2</sub>S. This reaction is similar to the four-electron sulfur oxidation of 1,4-dienes and styrenes that produces thiophenes and benzothiophenes, respectively (eqs 4 and 5).<sup>25</sup> Since the sulfur oxidation of **4** and **5** did not involve an oxidation state change of the metal or a change in the number of metal heteroatom bonds, these reactions can be classified using the degree of oxidation state method (DOX).<sup>25a,b</sup> The oxidation of

(24) (a) Caputo, R.; Ferreri, C.; Palumbo, G. *Synthesis* **1991**, 223–4. (b) Caputo, R.; Ferreri, C.; Palumbo, G. *Tetrahedron* **1986**, 42, 2369–76. (c) Wood, W. In *Trends in the Chemistry of 1,3-Dithioacetal, Organosulfur Chemistry, Synthetic Aspects* Page, P., Ed.; Academic Press: San Diego, CA, 1995; pp 133–224.

(25) (a) Klemm, L. H. *J. Heterocycl. Chem.* **1996**, 33, 569–74. (b) Klemm, L. H. *J. Heterocycl. Chem.* **1995**, 32, 1509–12. (c) Gronowitz, S. *The Chemistry of Heterocyclic Compounds; Thiophene and its Derivatives*; Gronowitz, S., Ed.; Interscience Publication, John Wiley and Sons: New York, 1960; Vol. 44; Part 1, pp 4–10 and references found within. (d) Broun, A. S.; Voronkov, G.; Shlyakhter, R. A. *Chem. Abstr.* **1949**, 43, 5392. (e) Arbuzov, B. A.; Kqtajev, E. G. *Dokl. Akad. Nauk. SSSR* **1954**, 96, 983–5. (f) Klemm, L. H.; Louris, J. N.; Boisvert, W.; Higgins, C.; Muchiri, D. R. *J. Heterocycl. Chem.* **1985**, 22, 1249–52. (g) Klemm, L. H.; Pou, S.; Detlefsen, W. D.; Higgins, C.; Lawrence, R. F. *J. Heterocycl. Chem.* **1984**, 21, 1293–6. (h) Klemm, L. H.; Karchesy, J. J.; McCoy, D. R. *Phosphorus Sulfur* **1979**, 7, 9–22. (i) Klemm, L. H.; Karchesy, J. J. *J. Heterocycl. Chem.* **1978**, 15, 561–3. (j) Klemm, L. H.; Karchesy, J. J.; Ross, R. *J. Heterocycl. Chem.* **1978**, 15, 773–5. (k) Klemm, L. H.; Karchesy, J. J. *J. Heterocycl. Chem.* **1978**, 5, 281–4. (l) Klemm, L. H.; McCoy, D. R.; Klopfenstein, C. E. *J. Heterocycl. Chem.* **1971**, 8, 383–89. (m) Klemm, L. H.; McCoy, D. R. *J. Heterocycl. Chem.* **1969**, 6, 735.

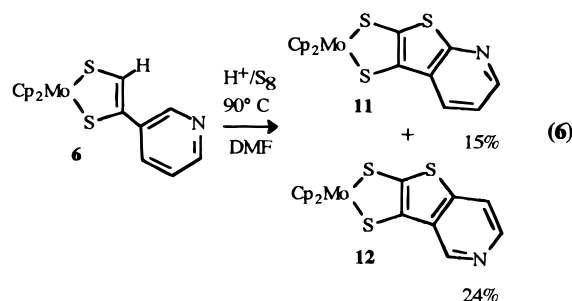
(22) (a) Gabe, E. J.; Le Page, Y.; Charland, J. P.; Lee, F. L.; White, P. S. *J. Appl. Crystallogr.* **1989**, 22, 384. (b) Sheldrick, G. M. *Acta Crystallogr.* **1990**, A46, 467.

(23) Harriman, A. *J. Chem. Soc., Faraday Trans. 1* **1980**, 76, 1978–85.

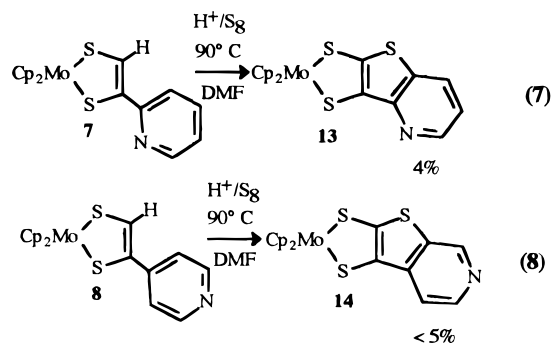


**4** and **5** has a  $\Delta(\text{DOX}) = 2$  consistent with a formal four-electron oxidation. The  $\Delta(\text{DOX})$  can be calculated by summing the number of carbon-heteroatom and carbon-carbon multiple bonds in the starting materials and products. Using this method the 1,2-dithiolate ligand has a  $\text{DOX} = 12$  (8 carbon-heteroatom bonds + 4 carbon-carbon multiple bonds) while the DSTQ ligand has a  $\text{DOX} = 14$  (10 carbon-heteroatom bonds + 4 carbon-carbon multiple bonds).

The  $S_8$  oxidation, eq 2, can be extended to the corresponding 3-pyridyl-substituted complex, **6** (eq 6). The 2,3-disulfidothienopyridine (DTTP) complexes, **11** and **12**, were the results



of oxidation at the 2- and 4-positions of pyridinium, respectively. Attempts to extend this reaction to the corresponding 2-pyridyl, **7**, 4-pyridyl, **8** (eqs 7 and 8), and several phenyl-substituted

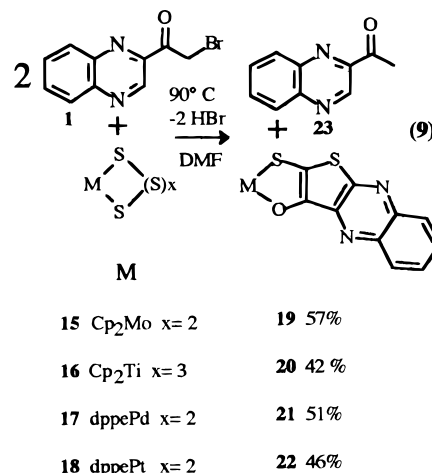


1,2-enedithiolates (not shown) of  $\text{Cp}_2\text{Mo}^{14}$  resulted in yields of the thiophene-containing products that were  $\leq 5\%$ . In these reactions (eqs 7 and 8) the starting material was consumed, over 24 h, and  $\text{Cp}_2\text{MoS}_4$  was generated as the major metal-containing product. No pyridine-containing compounds, other than the small amounts of **13** and **14**, were tolerant of neutralization and alumina chromatography. Of these complexes, only the 2,3-pyridyl derivative, **13** (eq 6), could be isolated in sufficient quantity and purity to be properly characterized.

Consistent with studies directed at the synthesis of thienopyridines and thienoquinolines where a sulfur radical is thought to be involved in the heterocycle oxidation,<sup>25l,m</sup> the generation of thiophenes from metallo-1,2-enedithiolates is dependent upon the site of heterocycle oxidation (eqs 6–8). Since the 2- and 4-positions of pyridinium are more susceptible to nucleophilic and radical attack than the 3-position, the yields of **13** and **14**, relative to the combined yield of **11** and **12**, support attack of the heterocycle by either a sulfur nucleophile or a sulfur-centered

radical.<sup>25,26</sup> This does assume that **13** and **14** are tolerant of the reaction conditions, which we have shown to be the case in separate experiments. The relatively high yields of the DSTQ derivatives are also consistent with the susceptibility of the 3-position of a 2-substituted quinoxaline to radical attack.<sup>3,26b</sup>

In addition to the DSTQ and DSTP derivatives, the 2-sulfido-3-oxidothienoquinoxaline (SOTQ) complexes, **19–22**, were prepared from the reactions of 1-(quinoxalin-2-yl)-2-bromoethanone with the respective polysulfido complexes (eq 9). Like



the corresponding DSTQ and DSTP derivatives, these complexes were air stable and, with the exception of **20**, were purified by column chromatography.

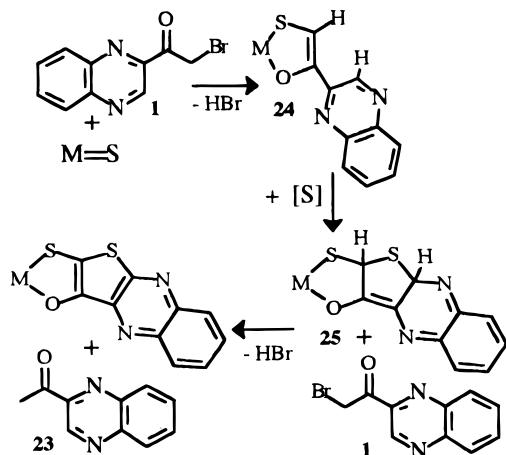
The conversion of the  $\alpha$ -bromo ketone, **1**, to the corresponding metal derivatives of SOTQ is also a four-electron oxidation that is accompanied by the loss of three protons and a bromide. In these reactions, two electrons are again required to generate the thiolate of the thiophene ring. The additional electrons and two protons are accommodated by the reduction of **1**, added in excess. The product of this reduction, 1-(quinoxalin-2-yl)-2-ethanone, **23**, could be isolated from the reaction mixture.<sup>21b</sup> The reduction of **1**, rather than the reduction of sulfur generated in these reactions, likely arises from the relative solubilities of these possible oxidants in DMF, the reaction solvent. Decreasing the moles of **1** lowers the yield of the SOTQ derivatives.

Like the reactions shown in eqs 2 and 4–8, the conversion of **1** to **19–22** has a  $\Delta(\text{DOX}) = 2$  consistent with a formal four-electron oxidation.<sup>25a,b</sup> Summing the number of carbon-heteroatom and carbon-carbon multiple bonds, **1** has a  $\text{DOX} = 12$  while the SOTQ ligand of the products, **19–22**, has a  $\text{DOX} = 14$ .

Given the reactivity of the quinoxaline-substituted metallo-1,2-enedithiolate complexes (eq 2), a 1-sulfido-2-oxido derivative, **24**, may be an intermediate in the synthesis of **19–22** (Scheme 1). We would envision such a complex resulting from an attack of the  $\alpha$ -bromo ketone by a metal sulfido or polysulfido complex. The reaction of **24** with sulfur and 1 equiv of **1** (an electron acceptor) would generate the observed products. Attempts to isolate **24** (on  $\text{Cp}_2\text{Mo}$ ) by limiting the amount of **1** in the reaction mixture accompanied by the addition of  $\text{PPh}_3$  as a sulfur scavenger were unsuccessful and resulted in reduced yields of the SOTQ derivative.

(26) (a) Barnes, R. A.; Brody, F.; Ruby, P. R. In *The Chemistry of Heterocyclic Compounds; Pyridines*; Klingsberg, E., Ed.; Interscience Publishers, Inc.: New York, 1960; Vol. 1; pp 1–29. (b) Simpson, J. C. E. In *The Chemistry of Heterocyclic Compounds; Condensed Pyridines and Pyrazines Rings*; Weissberger, A., Ed.; Interscience Publishers, Inc.: New York, 1953; pp 201–362.

Scheme 1

**Table 1.** Summary of X-ray Crystal Structure Data for Complexes **9** and **19**

	complex	
	<b>9</b>	<b>19</b>
formula	C <sub>20</sub> H <sub>14</sub> MoN <sub>2</sub> S <sub>3</sub>	C <sub>21</sub> H <sub>16</sub> Cl <sub>2</sub> MoN <sub>2</sub> OS <sub>2</sub>
fw	474.45	543.32
cryst system	monoclinic	orthorhombic
space group	P2 <sub>1</sub> /c	P2 <sub>1</sub> 2 <sub>1</sub> 2
<i>a</i> (Å)	10.766(1)	10.669(4)
<i>b</i> (Å)	14.385(1)	19.797(3)
<i>c</i> (Å)	11.983(1)	9.905(2)
$\alpha$ (deg)	90	90
$\beta$ (deg)	107.848(5)	90
$\gamma$ (deg)	90	90
<i>V</i> (Å <sup>3</sup> )	1766.6(2)	2092.0(9)
<i>Z</i>	4	4
$\rho_{\text{calc}}$ (g/cm <sup>-3</sup> )	1.784	1.726
<i>T</i> (K)	298	298
diffractometer	Siemens P4	Siemens P4
geometry	4-circle goniometer	4-circle goniometer
radiation, $\lambda$	Mo K $\alpha$	Mo K $\alpha$
abs coeff (mm <sup>-1</sup> )	1.035	1.096
<i>wR</i> <sub>2</sub> <sup>a</sup>	0.0792	0.0930
<i>R</i> <sub>1</sub> <sup>a</sup>	0.0331	0.0438
GOF <sup>a</sup>	1.042	1.142

<sup>a</sup> Residuals  $R_1 = \sum [|F_o| - |F_c|] / \sum |F_o|$ ,  $wR_2 = \{[\sum w(F_o^2 - F_c^2)^2] / \sum [w(F_o^2)^2]\}^{1/2}$ , where  $w^{-1} = [\sigma^2(F_o^2) + (0.0422P)^2 + 3.865P]$  and  $P = (\max(F_o^2, 0) + 2F_c^2)/3$ ,  $w^{-1} = [\sigma^2(F_o^2) + (0.1215P)^2 + 0.49698P]$ , and  $\text{GOF} = \delta = [\sum [w(F_o^2 - F_c^2)^2] / (n - p)]^{1/2}$ , where  $n$  = number of reflections and  $p$  = number of parameters.

**X-ray Crystallographic Results for 9 and 19.** Complexes **9** and **19** were the subject of single-crystal X-ray studies, the results of which are presented in Table 1 and shown in Figures 1 and 2. Both **9** and **19** contain an extended planar thiophene ligand with no atoms deviating from the least-squares plane by more than 0.03 Å. In complex **19**, the Mo–S and Mo–O bond distances of 2.464(5) and 2.086(9) Å are best described as single bonds. The C(11)=C(12) bond in **19** was 1.28(2) Å, while that of the 2,3-dithiophene complex **9** was 1.363(5) Å and the metallo-1,2-enedithiolate complex **4** was 1.339(7) Å.<sup>14</sup> The O(1)–C(12) bond of **19** is 1.29(2) Å. The O–Mo–S(1) bond angle of 81.2(3)° in **19** was not significantly different from the S–Mo–S bond angle of 83.65(3)° in **9**. However, the Mo–O–C(12) angle of 116.5(13)° and the Mo–S(1)–C(11) bond angle of 94.3(7)° of **19** were significantly different from the Mo–S–C angles found in **9**, which were 104.05(11) and 104.09(11)°, and those of **4**, which were 105.68(18) and 106.62-

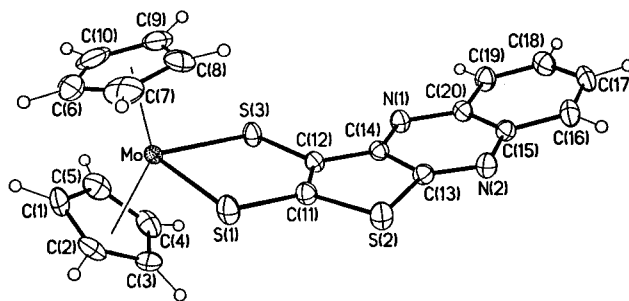


**Figure 1.** ORTEP drawing of **9** with the thermal ellipsoids drawn at 50% probability. Selected bond lengths (Å) and angles (deg) are as follows: Mo–S(1), 2.4729(10); Mo–S(3), 2.4821(9); S(1)–C(11), 1.726(3); S(2)–C(11), 1.763(3); C(11)–C(12), 1.363(5); C(12)–C(14), 1.431(4); C(11)–S(3), 1.764(4); C(13)–S(2), 1.746(3); C(13)–C(14), 1.445(4); S(1)–Mo–S(3), 83.61(3); Mo–S(1)–C(11), 104.05(11); Mo–S(3)–C(12), 104.09(11); S(1)–C(11)–C(12), 125.0(2); S(3)–C(12)–C(11), 123.0(2); S(1)–C(11)–S(2), 120.4(2).

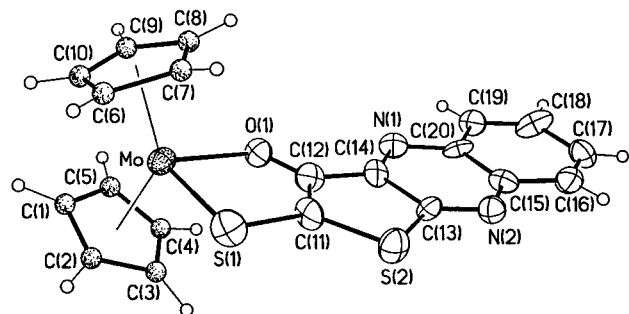


**Figure 2.** ORTEP drawing of **19** with the thermal ellipsoids drawn at 50% probability. Selected bond lengths (Å) and angles (deg) are as follows: Mo–O(1), 2.088(9); Mo–S(1), 2.468(5); S(1)–C(11), 1.75(2); O(1)–C(12), 1.29(2); C(11)–C(12), 1.28(2); C(12)–C(14), 1.45(2); C(11)–S(2), 1.77(2); C(13)–S(2), 1.74(2); C(13)–C(14), 1.47(2); O(1)–Mo–S(1), 81.0(3); Mo–S(1)–C(11), 94.3(7); Mo–O(1)–C(12), 117.4(13); S(1)–C(11)–C(12), 120.2(2); S(1)–C(11)–S(2), 122.6(13).

(16)°.<sup>14</sup> Similar differences in bond angles were seen in vanadium thiophenol complexes<sup>27</sup> and the platinum 1-enol-2-selenate complex (PPh<sub>3</sub>)<sub>2</sub>Pt[OSEc<sub>2</sub>{Me}{C(O)Me}].<sup>28</sup> The thiophene rings in **9** and **19**, while essentially planar, were distorted in that the C(11)=C(12) bond distances at 1.363(5) and 1.28(2) Å, respectively, were considerably shorter than both the C(12)–C(13) and the C(13)–C(14) bonds that were both ≈1.45 Å.

**UV–Visible Spectroscopy and Electronic Transitions.** All of the complexes prepared in this study have an acid-sensitive band assignable to an intraligand (IL) transition. This transition was thought to possess considerable thiolate to heterocycle  $\pi^*$  character and was similar to an ILCT transition in complexes **4–8**.<sup>14,15</sup> In complexes **9** and **19** this band is found at 532 nm (18 800 cm<sup>-1</sup>) and 536 nm (18 660 cm<sup>-1</sup>), respectively (Figure 3). Upon protonation of the quinoxaline moiety, this band is red-shifted by 3810 and 3390 cm<sup>-1</sup>, respectively (Table 2).

Like **9** and **19**, the palladium complexes, **10** and **21**, have similar bands at 476 nm (21 010 cm<sup>-1</sup>) and 518 nm (19 310 cm<sup>-1</sup>) that are red shifted by 4671 and 3381 cm<sup>-1</sup> upon protonation, respectively. The energy of the IL transition is nearly equivalent in the palladium complex, **21**, and the platinum complex, **22**, supporting the IL assignment. If this transition had considerable d to d, MLCT, or LMCT character, it would be substantially more sensitive to the Pt for Pd exchange.<sup>29–33</sup>

(28) Yamazaki, S.; Deeming, A. J. *Polyhedron* **1996**, *15*, 1847–52.

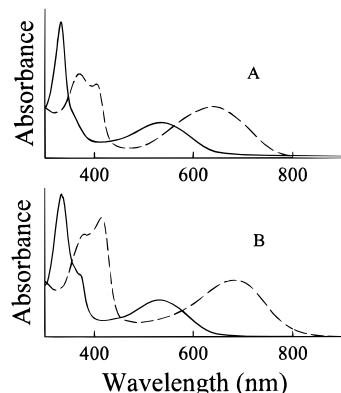
(29) Shupack, S. I.; Billig, E. C.; Williams, R.; Gray, H. B. *J. Am. Chem. Soc.* **1964**, *86*, 4594–602.

(30) Gray, H. B.; Ballhausen, C. J. *J. Am. Chem. Soc.* **1963**, *85*, 260–4.

(27) Klich, P. R.; Daniher, A. T.; Challen, P. R.; McConville, D. B.; Youngs, W. J. *Inorg. Chem.* **1996**, *35*, 347–56.

**Table 2.** UV–Visible Absorption Bands of the Neutral and Protonated 2,3-Sulfidothiophene and 2-Sulfido-3-oxidothiophene Complexes

complex	$\lambda_{\max}$ ( $\epsilon$ ) neutral complexes	$\lambda_{\max}$ ( $\epsilon$ ) protonated complexes
<b>9</b>	334 (13 830), 371 (sh) (6020), 532 (3540)	381 (10 260), 414 (11 840), 681 (5790)
<b>10</b>	326 (10 280), 376 (6820), 476 (5610)	352 (8710), 432 (9980), 612 (7760)
<b>11</b>	290 (sh, 4870), 358 (3950), 529 (660)	305 (4550), 388 (2910), 490 (sh, 940)
<b>12</b>	296 (7900), 376 (3110), 531 (820)	334 (10530), 388 (3520), 532 (3050)
<b>19</b>	332 (15 050), 536 (3510)	371 (11 930), 404 (11 840), 655 (5790)
<b>20</b>	328 (8320), 429 (1840), 482 sh (1000), 562 (sh 340)	344 (6220), 396 (sh 2620), 422 sh (2040), 526 (1440)
<b>21</b>	332 (30 590), 358 sh (9380), 370 sh (6470), 518 (5420)	360 (15 070), 409 (12 810), 628 (7580)
<b>22</b>	327 (32 700), 357 sh (9410), 370 sh (8150), 501 (6270)	356 (11 290), 415 (13 790), 614 (8870)

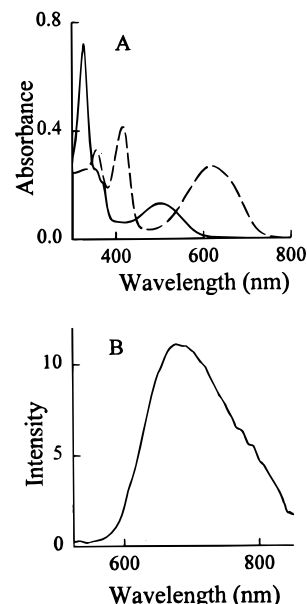
**Figure 3.** UV–vis absorption spectra of (A) **19** and **19H**<sup>+</sup> in DMSO and (B) **9** and **9H**<sup>+</sup> in DMSO. Solid lines are the absorbance spectra of the neutral complex, while the dashed lines are the absorbance spectra of the protonated complexes.

On the basis of its acid sensitivity, the IL transition of **20** is assigned to a band at 482 nm ( $20\,750\text{ cm}^{-1}$ ). This band is red shifted upon protonation by  $\approx 1740\text{ cm}^{-1}$ . Unlike the molybdenum, palladium, and platinum SHTQ derivatives, the IL transition is not the lowest energy band of the  $\text{Cp}_2\text{Ti}$  derivative. The lowest energy band, at 560 nm, was assigned to a LMCT transition.<sup>18,34</sup>

Like **20**, the IL transitions of **11** and **12** (found at 358 and 376 nm, respectively) are not the lowest energy bands. These findings are consistent with those of the 3-pyridyl-substituted 1,2-enedithiolate complex,  $\text{Cp}_2\text{Mo}\{\text{S}_2\text{C}_2(3\text{-pyridine})(\text{H})\}$ , **6**,<sup>14</sup> where the lowest energy band was assigned to a LMCT transition.

**Luminescence Spectra of 22.** Excitation of solutions of  $\text{dppePt}\{\text{S}_2\text{C}_2(\text{heterocycle})(\text{H})\}$ , where heterocycle = 2-quinoxaline<sup>13</sup> and 2- and 4-pyridinium,<sup>15</sup> lead to room-temperature emissions. All of these complexes have as their lowest energy band an ILCT transition. Consistent with these findings, excitation of solutions of **22** lead to a broad emission with little vibronic fine structure (Figure 4). The emission intensity was linear with concentration, and the excitation profile was identical to the absorption spectra of **22**. The quantum yield and emission maxima were both solvent sensitive (Table 3). The quantum yield increased 50 times and the emission maxima red shifted by  $\approx 2000\text{ cm}^{-1}$  as the solvent polarity increased from  $\text{CCl}_4$  to DMSO. This suggests that the excited states may have some charge transfer character.

Luminescent lifetime measurements of deaerated solutions of **22** provided frequency plots that were best fit as a sum of two exponential decays with one lifetime in the 6 ns range and one lifetime in the 0.3 ns range (Table 3).

**Figure 4.** (A) UV–vis absorption spectra of **22** and **22H**<sup>+</sup> in DMSO. (B) Air-free emission spectrum of **22** in DMSO. The solid lines are the absorbance and emission spectra of the neutral complex, while the dashed line is the absorbance spectra of the protonated complex.**Table 3.** Solvent Dependence of the Luminescence Maxima, Quantum Yield, and Lifetimes of **22**

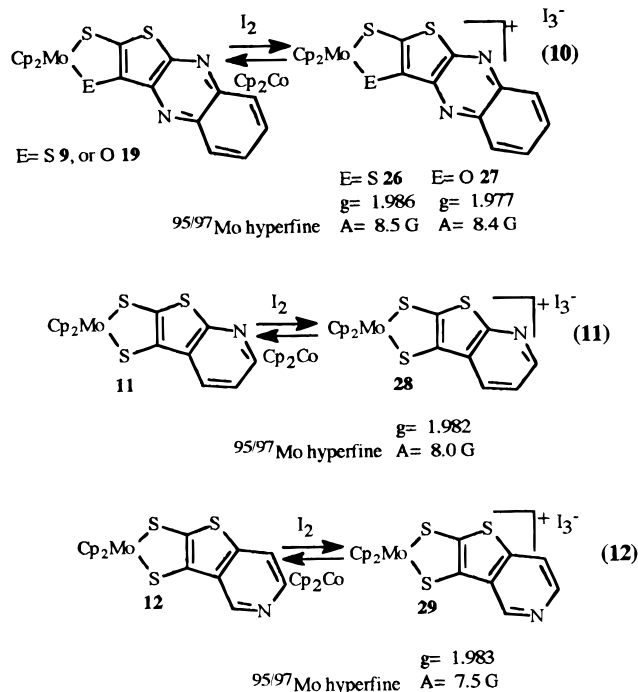
solvent	$\phi^a$	$\lambda$ (nm)	$\tau$ (ns)
DMSO	0.005	690	5.94 (3) 0.26 (8)
DMF	0.003	681	
acetone	0.0009	670	
$\text{CH}_2\text{Cl}_2$	0.0008	668	
$(\text{CH}_2\text{Cl})_2$	0.0008	663	5.67 (1) 0.27 (9)
dioxane	0.0005	651	
toluene	0.0003	648	
$\text{Et}_2\text{O}$	0.0002	611	
$\text{CCl}_4$	0.0001	602	

**Electrochemistry and EPR Measurements.** The molybdenum DSTQ and SOTQ complexes, **9** and **19**, have reversible electrochemistry with oxidation waves centered at 420 and 378 mV in  $\text{CH}_2\text{Cl}_2$ , respectively. The protonation of these complexes lead to a positive shift in the  $E_{1/2}$  of  $\approx 75\text{ mV}$  for both complexes. The difference in the  $E_{1/2}$  values for **9** and **19** is 42 mV, a value typical for a thiolate–alkoxide ligand exchange on a  $\text{Mo}^{\text{IV}}$  center.<sup>35,36</sup> Complexes **11–13** also have reversible electrochemistry with oxidation waves that were centered at 260, 272, and 389 mV, respectively. Protonation of the heterocycle in these complexes shifts the  $E_{1/2}$  by 150–200 mV.

Oxidation of complexes **9**, **11**, **12**, and **19** with  $\text{I}_2$  (or  $\text{Br}_2$ ) lead to the generation of **26–29**, respectively (eqs 10–12).

(31) Werden, B. G.; Billig, E.; Gray, H. B. *Inorg. Chem.* **1966**, 5, 78.  
 (32) Fackler, J. P., Jr.; Coucouvanis, D. *J. Am. Chem. Soc.* **1966**, 88, 3913–20.  
 (33) Bowmaker, G. A.; Boyd, P. D. W.; Campbell, G. K. *Inorg. Chem.* **1983**, 22, 1208–13.  
 (34) Bolinger, C. M.; Rauchfuss, T. B. *Inorg. Chem.* **1982**, 21, 3947–54.

(35) Roberts, S. A.; Young, C. G.; Kipke, C. A.; Cleland, W. E.; Yamanouchi, K.; Carducci, M. D.; Enemark, J. H. *Inorg. Chem.* **1990**, 29, 3650–6.  
 (36) Harlan, E. W.; Berg, J. M.; Holm, R. H. *J. Am. Chem. Soc.* **1986**, 108, 6992–7000.



Complexes **26–29** were stable in deaerated solutions for several hours and could be reduced to **9**, **11**, **12**, and **19**, respectively, with  $\text{Cp}_2\text{Co}$  in an overall yield for the two reaction steps of  $\geq 90\%$ .

The room-temperature EPR spectra of **26–29** in  $\text{CH}_2\text{Cl}_2$  solution were characterized by  $g$  values at  $\approx 1.98$  and  $^{95/97}\text{Mo}$  hyperfines of  $\leq 8.5 \text{ G}$ . While similar hyperfine couplings to  $^{95/97}\text{Mo}$  were observed for  $[\text{Cp}_2\text{Mo}\{\text{S}_2\text{C}_2(\text{heterocycle})(\text{C}(\text{O})\text{Me})\}]^+$  (heterocycle = pterin and quinoxaline),<sup>1</sup> these values were much smaller than the 36 G hyperfine observed for  $[\text{Cp}_2\text{MoCl}_3]^+$ .<sup>37</sup> The small  $^{95/97}\text{Mo}$  hyperfine suggests that the electron in **26–29** is substantially delocalized throughout the ligand. The small hyperfine couplings to molybdenum supports the description of **26–29** not as  $\text{Mo}^{\text{V}}$  complexes but as ligand-centered radical cations. The lack of  $^{14}\text{N}$  hyperfine suggests that the semi-occupied molecular orbital is primarily dithiolato–thiophene- or thiolato–hydroxo–thiophene-based.

## Conclusion

Metallo-1,2-enedithiolates of the type  $\{\text{MS}_2\text{C}_2(\text{R})(\text{H})\}$ , where  $\text{R}$  = heterocycle, are susceptible to chemical oxidation by sulfur. The product from this oxidation was trapped by an appended

heterocycle generating the 2,3-sulfidothiophene ligand. These reactions (eqs 2 and 5) are reminiscent of the four-electron ( $\Delta(\text{DOX}) = 2$ ) sulfur oxidation of 1,4-dienes and styrenes that produce thiophenes and benzothiophenes, respectively (eqs 4 and 5). The reaction of the heterocyclic substituted 1,2-enedithiolate with sulfur is sensitive to the position of the heterocycle that is oxidized in the reaction. Product yields suffered when the site of oxidation is not activated toward radical attack. As such, the disulfidothiophene derivatives were obtained in the best yields when the site of oxidation was either two or four to the nitrogen of the protonated heterocycle. These findings are consistent with studies directed at the synthesis of thienopyridines and thienoquinolines that require attack of the heterocycle by a radical center.<sup>251,m</sup>

Many of the properties of the 2,3-disulfidothienoquinoxaline, 2,3-disulfidothienopyridine, and 2-sulfido-3-oxidothienoquinoxaline complexes were similar to those of 2,3-sulfidoquinoxaline complexes.<sup>11,38</sup> The synthetic methods outlined in this paper should allow a range of these complexes to be prepared that include a variety of heterocyclic groups that may share these general properties. Thus, the properties of these complexes could be fine tuned, a particularly useful feature in the design and synthesis of new lumiphores.<sup>10–13,15,38a</sup> The intraligand transition in **22** serves as a luminescent chromophore, and **22** is a member of an emerging class of platinum thiolates that are emissive at room temperature in solution.

In addition to serving as a chromophore, the 2-sulfido-3-oxidothienoquinoxaline ligand, along with the 2,3-sulfidothienoquinoxaline and 2,3-sulfidothienopyridine ligands, stabilize the radical generated by the oxidation of the corresponding molybdenum complexes. The small molybdenum hyperfine clearly demonstrates that the semi-occupied molecular orbital in these oxidized complexes is localized primarily on the ligand and not the metal center.

**Acknowledgment.** We are indebted to the donors of the Petroleum Research Fund, administered by the American Chemical Society (Grant No. 28499-G3), and the Exxon Education Foundation for supporting this work.

**Supporting Information Available:** Tables listing data collection details, crystallographic data, positional parameters, anisotropic thermal parameters, and bond lengths and angles for **9** and **19** (13 pages). Ordering information is given on any current masthead page.

IC961428V

(37) Cooper, R. L.; Green, M. L. H. *J. Chem. Soc. A* **1967**, 1155–60.

(38) (a) Cummings, S. D.; Eisenberg, R. *Inorg. Chem.* **1995** *34*, 2007–14. (b) Theriot, L. J.; Ganguli, K. K.; Kavarnos, S.; Bernal, I. *J. Inorg. Nucl. Chem.* **1969**, *31*, 3133–40. (c) Boyde, S.; Garner, C. D. *J. Chem. Soc., Dalton Trans.* **1991**, 713–16.